Change detection of groundwater level and quality in coastal aquifers of Malabar region in Kerala, India

Abstract

A study was conducted to assess the changes in groundwater level and quality for the period 2005-2020 in the coastal aquifer of the Vatakara-Koyilandy stretch in the Kozhikode district of Kerala. Hydrogeochemical analysis of groundwater quality parameters, irrigation water quality analysis and preparation of spatial variability of groundwater level and salinity were used for the study. The Piper diagram was used to track the change in the hydrochemical parameters of groundwater sources in 2005 and 2020 and identify changes in the chemical facies of the groundwater. The Gibbs diagram was used to identify the source of the dissolved ions present in the groundwater in both years. The United States Salinity Laboratory diagram was used to assess the groundwater's suitability for irrigation. The spatial variation of water table elevation and salinity were compared using the ordinary kriging method of interpolation. An increase in seawater intrusion into the wells and a reduction in irrigation water quality was indicated by the change in the Hydrochemical facies, and the shifting of more groundwater samples in the evaporation dominance zone in the Gibbs plot. The spatial variability of groundwater level indicates a reduction in premonsoon in both years. On the North coast, a 4% increase in the area under groundwater level < 2m. the reduction in the groundwater table on the coast increases the chance of sweater intrusion and thereby increased salinity. Even though the study area receives heavy rainfall during monsoon and recharging of the coastal aquifer, seawater intrusion progressed landward from 2005 to 2020 during the premonsoon and affected the groundwater level and quality over this period.

Keywords: Aquifer characterisation, Hydrochemical analysis, Spatial prediction, Groundwater, Seawater intrusion

1. INTRODUCTION

Groundwater is a dynamic and replenishing natural resource. There has been an increase in groundwater extraction as a result of the sharp rise in demand for agricultural, industrial, and home uses. Both the quantity and quality of groundwater are declining in most of India. The issue appears to be more severe when the land meets the sea, especially coastal aquifers. Unsustainable groundwater extraction brought on by growing urbanisation contributes to ecological and environmental problems such as coastal erosion, ground subsidence, seawater intrusion, and coastal floods. (Michalopoulos and Dimitriou, 2018). Studies of the spatial distribution of groundwater quality and level over time can help identify vulnerable locations and shed light on how the problem's geographic scope varies over time.

Groundwater statistical analysis, spatiotemporal variability of the issue, and the relevance of trends in data with seasonality are all very helpful in identifying changes and predicting projections for the future. Hydrochemical facies, mechanisms

governing groundwater chemistry, saltwater intrusion status in agriculture, development of a water quality index, and major cation and anion interpolation are a few frequent analyses to look into the geochemical process, source of contamination, and irrigation suitability of groundwater. Using the Gibbs diagram, it is common practice to thoroughly analyse geochemical processes and the mechanisms that control them.

The spatial variability map of groundwater depth and quality indicators for the National Capital Territory of Delhi, India, was created by Dash et al., (2010). The geographic variability of groundwater depth and quality was investigated using ordinary kriging. The semivariogram parameters were found to fit well in both the exponential and spherical models for water depth and water quality parameters. Based on data from 97 wells monitored over 7 years, Arslan, (2012) conducted spatial and temporal assessments of groundwater salinity in Bufra Palin, Turkey. ArcGIS Geostatistical Analyst used an explanatory data analysis, semivariogram model selection, cross-validation, and the generation of a groundwater salinity distribution pattern. Ordinary Kriging (OK) was used to investigate groundwater salinity variations over time, whereas Indicator Kriging (IK) was utilised to investigate groundwater salinity about pollution threshold values. With a total of 123 water samples, including 105 unconfined groundwater samples, Zhang et al., (2012) investigated the hydrogeochemical characteristics of groundwater in the Delingha area, northwest China. Hydrochemical types in groundwater were studied using the Piper diagram. Gibbs diagram was used to identify hydrogeochemical evolution, which involves precipitation, rock weathering, and evaporation–crystallization processes. The findings revealed that groundwater hydrochemistry had a distinct zoning pattern in this location.

To determine the suitability of groundwater for irrigation and drinking, a hydrogeochemical analysis was conducted in and around the Veeranam tank region by Sathiamoorthy and Ganesan, (2018). The Sodium Percentage, Wilcox Diagram, Alkalinity and Salinity Hazard, Magnesium Hazard, and Residual Sodium Carbonate are used to determine the irrigation water quality. They categorized the samples according to the Wilcox and USSL classifications. Lanjwani et al., (2021) used ArcGIS 10.5 to map the spatial variation of groundwater quality in Larkana of Sindh, Pakistan using the IDW method. The water quality index (WQI) was created to categorise suitability for drinking based on various parameters.

The objective of this study is to assess the changes in groundwater level and quality for the period 2005-2020 by analysing the pre- and post-monsoon trends, preparing the spatial prediction maps, studying the hydrochemical types, hydrogeochemical evolution, and preparing the irrigation water quality index.

2. MATERIALS AND METHODS

2.1 Study Area

The study area is situated in the north part of Kerala's Kozhikode coast, the central part of the Malabar coast in India. The study area lies between 750 73'-750 62' East longitudes and 110 42'-110 56' North latitudes with a total area of 270 km^2 (Fig.1). the climate of this study area is tropical and humid with an average annual rainfall of 2700 mm out of this, 60 % is received during the South-west monsoon and 25% is received during the North-East monsoon. The rest of the rainfall occurs in

other seasons. December-January to March-April are the dry months. The study area has a humid tropical climate with an average temperature of 27° C.

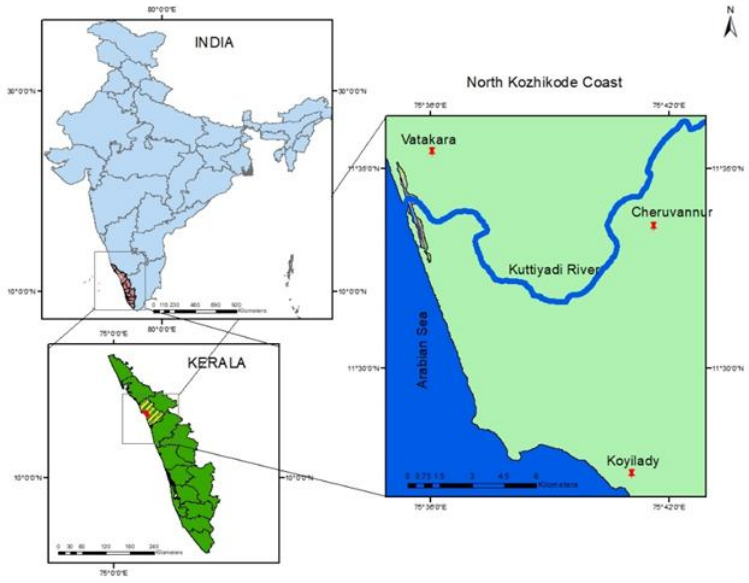

Fig. 1 Study area location map

2.2 Geology

The various geological formations in the study area comprise alluvium deposits that are underlain by laterite and sedimentary rocks, mostly charnockites with mafic granulite enclaves. Laterites occur as capping of these rocks which formed as the as a residue of tropical weathering of crystalline rocks. Groundwater in weathered crystallines is present under unconfined conditions and semi-confined in deep crystalline formations. Groundwater table depth ranges from 0.73 m to 16.11 m below ground level (CGWB, 2013). The well logs of representative wells suggest aquifer consists of three layers namely; the top unconfined layer, an aquitard and a semi-confined aquifer at the bottom.

2.3 Geomorphology and soil types

The geomorphology of Kozhikode district can be categorised as a coastal region in the west, midland in the central part and highland in the east. The study area was delineated with elevation within 10 m from MSL extending over the coastal region and midlands. The soil types in the region are coastal alluvial soil in coastal plain and in low-lying areas, riverine alluvial soil along riverbanks, red loam soil and brown hydromorphic soil (KSPCB, 2019; Nair, 1987; Nazimuddin, 1993). The alluvium deposits are underlain by laterite and sedimentary rocks, mostly charnockites with mafic granulite enclaves. The coastal zone is covered by excessively drained to moderately drained sandy deposits, and the alluvium deposits are covered by excessively drained to moderately drained sandy deposits (CGWB, 2013; KSPCB, 2019; Salaj et al., 2018). The soil conditions are ideal for growing coconuts, spices, and plantation crops, and are average for other crops. Coconut, spices, paddy and plantation crops are the most important crops cultivated in the study area.

2.4 Frequency analysis of rainfall

The present study uses 100-year continuous rainfall data acquired from IMD gridded data. The Weibull Plotting position formula was applied to the rainfall data to compute the probability of rainfall's exceedance of rainfall. The probability of exceedance of rainfall is

$$T = \frac{m}{(N+1)} \quad (1)$$

given by,

where m is the order or rank and N is the total number of events

2.5 Log-normal distribution

The maximum rainfall for a particular return period was calculated using the log-normal distribution which is a probability distribution of a random variable whose logarithm is normally distributed. The following equation was used to compute the maximum rainfall for a particular return period

$$XT = Xav + k\sigma \quad (2)$$

Where X_{av} is the mean value, k is the frequency factor and

σ is the standard deviation and N is the sample size and the value of k is

$$\sigma = \left[\frac{\Sigma(Xi - Xavg)2}{N-1}\right]^{1/2} \quad (3)$$

determined considering the coefficient of skewness as zero.

2.6 Hydrogeochemical Analysis

Data on the concentration of major ions such as $HCO3^-$, Cl^-, Ca^{2+}, Mg^{2+}, Na^+, etc K^+ were used for hydrochemical analysis using the Piper diagram. The trilinear Piper diagram proposed by (Piper, 1944), was applied to plot the concentration of major cations and anions to determine changes that occurred on the chemical facies of the groundwater in 2005 and 2020 to identify the evolution of hydrochemical parameters of groundwater sources in this period. The Trilinear Piper diagram was constructed with the help of Geochemical analyst software version 2015.1.14.

Gibb's diagrams are a tool for understanding groundwater chemistry's various mechanisms and processes (Gibbs, 1970). The source of the dissolved ions in the groundwater can be understood by the Gibbs diagram which is a plot of $(Na^+)/(Na^+ + Ca^{2+})$ vs TDS and $Cl^-/(Cl^- + HCO_3^-)$ vs TDS. Gibbs diagram was prepared for the years 2005 and 2020 with the help of GRAPHER software.

2.7 Irrigation Water Quality

The United States Salinity Laboratory diagram (USSL diagram) for the suitability of water for agricultural uses was used to determine the suitability of groundwater for irrigation. Sodium percentage determines the ratio of sodium to the total cations viz.,

sodium, potassium, calcium and magnesium. The diagram for the years 2005 and 2020 were prepared using GRAPHER software.

SAR was prepared using the following formulae

$$SAR = \frac{Na^{+}}{\frac{\sqrt{Ca^{2+} + Mg^{2+}}}{2}} \quad (4)$$

Where, the ionic concentrations are expressed in meq/l.

2.8 Spatial Variation of Groundwater Level and Salinity

Geostatistical tools were used to describe the spatial variability of groundwater levels and salinity. Ordinary kriging was used to plot the spatial variability map of groundwater salinity and levels (Isaaks and Srivastava, 1989).

3. RESULTS AND DISCUSSION

3.1 Rainfall Extreme Probability Analysis

The method of rainfall extreme probability analysis was used to examine the maximum annual rainfall. The maximum rainfall depths for various return periods are presented in Fig. 2, those were calculated using the Plotting Position Formula (Sabarish et al., 2017) and the variation of annual rainfall is presented in Fig. 3. According to the analysis of the annual rainfall for various return periods, the annual rainfall between the 50- and 100-year return periods differs by 180 mm. For the 10-, 30-, and 100-year return periods, the annual rainfall values are 3000, 3019, and 3214 mm, respectively.

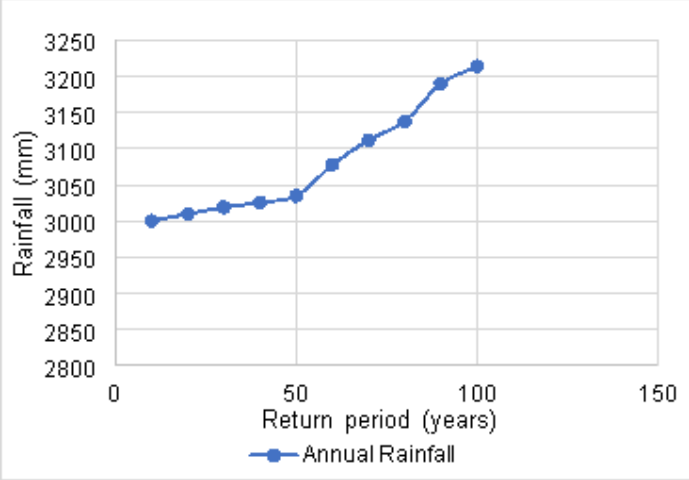

Fig. 2 Maximum annual rainfall Vs Return Period

50% of the land in Kerala is hilly or ghat dominated and the west is bounded by the Arabian sea. The results showed that the district is highly vulnerable to heavy rainfall. The heavy rain during the monsoon, or a low-pressure area, and interaction

from wind from the sea. Heavy rainfall in the fragile ecosystem with laterite soil will cause damage to the ecosystem.

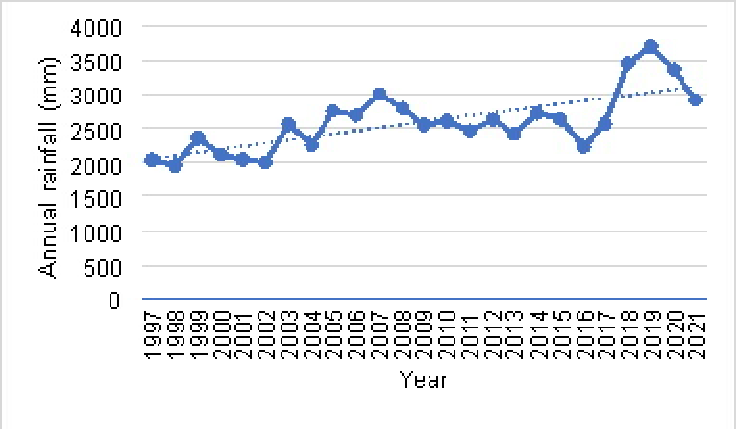

Fig. 3 Variation of annual rainfall during the 15 years

3.2 Statistical summary of groundwater level and salinity

The statistical summary of groundwater level and salinity were given in Table 1. The minimum groundwater elevation in the study area was -0.23 m in 2005 and reduced to -0.61 m in 2020. The corresponding EC values were 0.87 dS/m and 0.96 dS/m. The mean values of EC were 1.96 dS/m in 2005 and 2.61 dS/m in 2020. This indicates a direct relationship between groundwater salinity with the reduced groundwater level in the area. The mean value of pH in both years resulted in 7.9.

Table 1. Statistical summary of groundwater level and salinity in the study area

	GW level	TDS	EC	pH
2005				
Minimum	-0.23	0.22	0.67	7.6
Maximum	6.35	2.83	3.18	8.6
Mean	3.73	1.13	1.96	7.9
STDV	1.09	0.48	0.52	0.6
2020				
Minimum	-0.61	0.49	0.96	7.5
Maximum	5.58	2.95	3.96	8.7
Mean	3.01	1.87	2.61	7.9
STDV	1.22	0.47	0.51	0.5

GW level: Groundwater level (m), TDS: Total Dissolved Solids (kg/m^3), EC: Electrical conductivity (dS/m)

3.3 Hydrogeochemical analysis

3.3.1 Piper diagram

The Hill–Piper trilinear diagram (Piper, 1944), consists of triangle and diamond-shaped fields with subdivisions representing the various water types and hydrochemical facies that existed in the aquifer (Ali and Ali, 2018). These hydrogeochemical facies present in the aquifer for the years 2005 and 2020 shed light on the changes that occurred in the geochemical process influencing the groundwater quality in the aquifer (Fig.4).

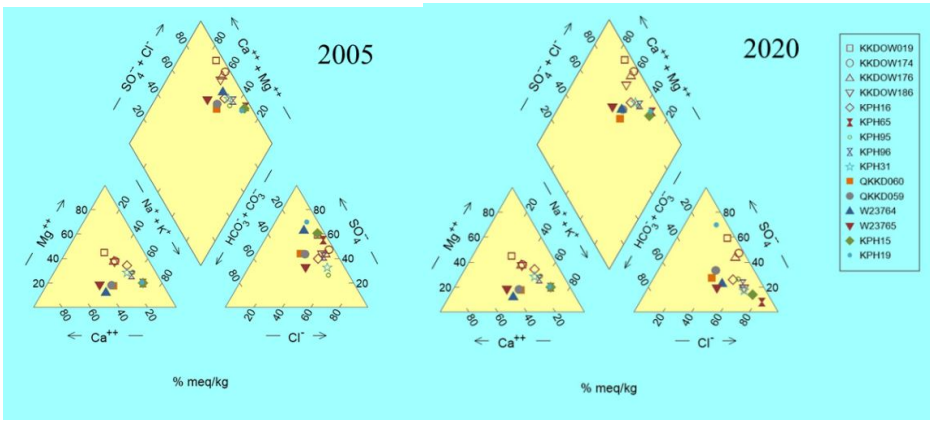

Fig. 4 Hydrochemical facies in 2005 and 2020

From the cationic triangular field of the Piper diagram in 2005, 45% of the samples fall into the no dominant type, conversely, 55% of these groundwater samples fall Sodium or Potassium type. A few samples were under the Ca^{+} dominant type, remaining placed under Na^{+} and K^{+} dominant regions. In the anionic triangular field, 30% of the samples fall into the no-dominant type, and the rest 70 % of the samples are scattered into the chloride type and sulphate type region. In the year 2020, the groundwater samples fall in the cationic triangle in a similar pattern as in 2005; conversely, most of the samples shifted to chloride type in the anionic triangle. Hydrogeochemical facies in 2020 are Na-Cl followed by Ca-Mg-Cl. This indicated the seawater intrusion in the study area (Alfarrah et al., 2011; Shin et al., 2020). Groundwater samples of no-dominant type were affected by seawater intrusion by 2020.

3.3.2 The mechanism governing groundwater chemistry

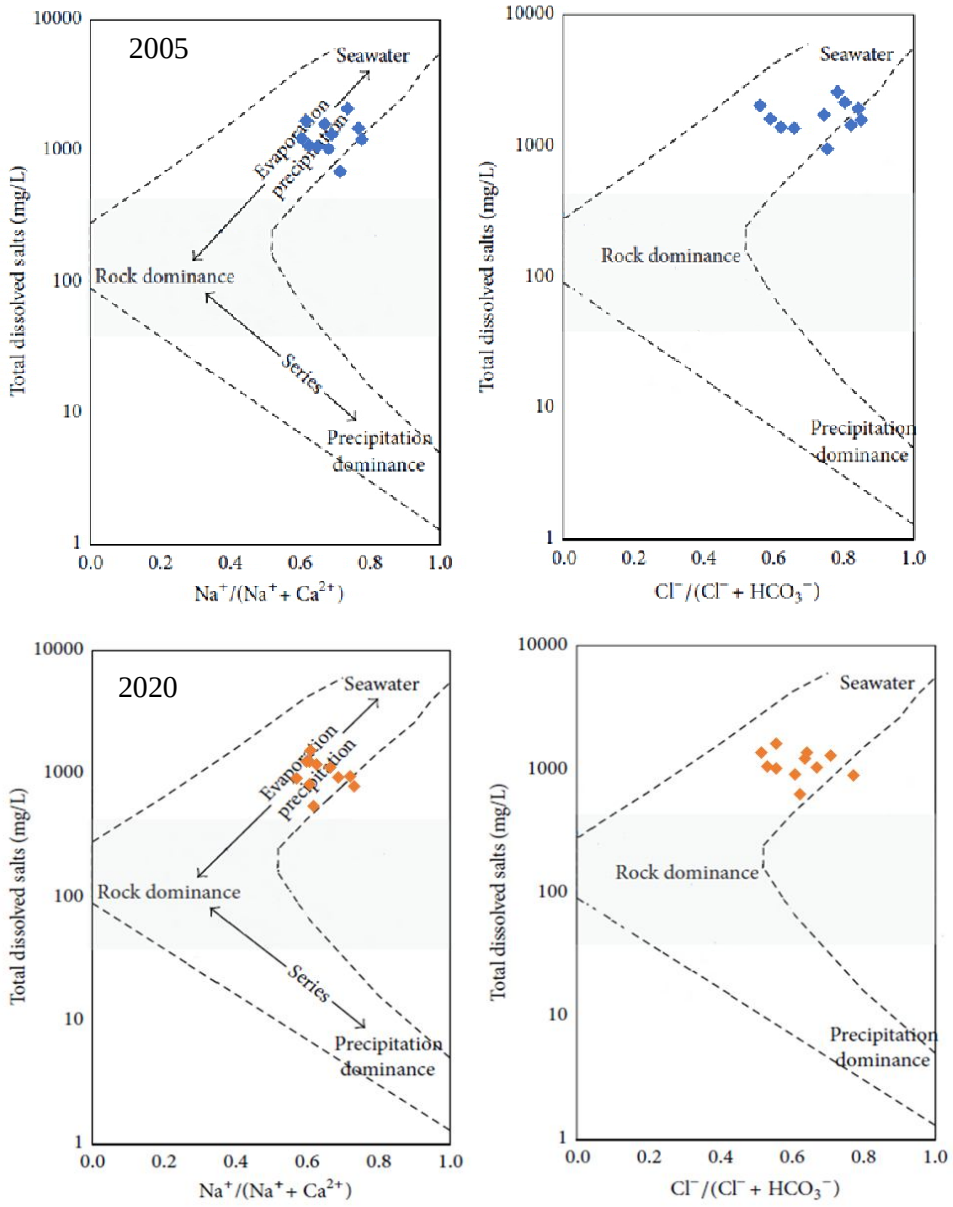

Fig. 5 Gibbs diagram in 2005 and 2020

The diagram which expressed the mechanism that controls the chemical composition of major dissolved salts in the groundwater was described using the Gibbs Diagram. The chemical data of groundwater from unconfined and semiconfined aquifers were plotted in the diagram (Fig. 5). Most of the aquifer samples, according to Gibb's analysis, were found to be in the evaporation-dominating zone in both the 2005 and 2020 time periods, indicating that evaporation dominance is primarily responsible for the groundwater chemistry in aquifers.

Most of the samples have large quantities of Cl-, which suggests that Cl- ions can come from a variety of sources. The distribution of Na+ ions is concentrated

largely at high proportions, suggesting that all Na+ ions are formed from the same source or by the same geological process(Rao et al., 2017). In the aquifer, saltwater produces the ions Na^+ and Cl^- and the evaporation dominance on the diagrams shows seawater intrusion in the aquifer (Lanjwani et al., 2022; Sangadi et al., 2022).

3.4 Irrigation water quality

United States Salinity Laboratory diagram (USSL diagram) is an approach to finding the groundwater quality for agriculture purposes, which was applied to realize the groundwater parameters (Richards, 1954). The results of the USSL diagram (Fig. 6) illustrate that most of the groundwater samples fall in the category of C3S2 (high salinity with medium sodium followed by C4S2 (very high salinity with medium sodium). The electrical conductivity ranges from 1.87 to 4.2 dS/cm and SAR values range from 12 to 18. The result reveals that there is an occurrence of medium alkalinity and high to very high salinity hazards in the aquifer. The groundwater is not suitable for irrigation due to the presence of high salinity and little danger of exchangeable sodium (Ali and Ali, 2018).

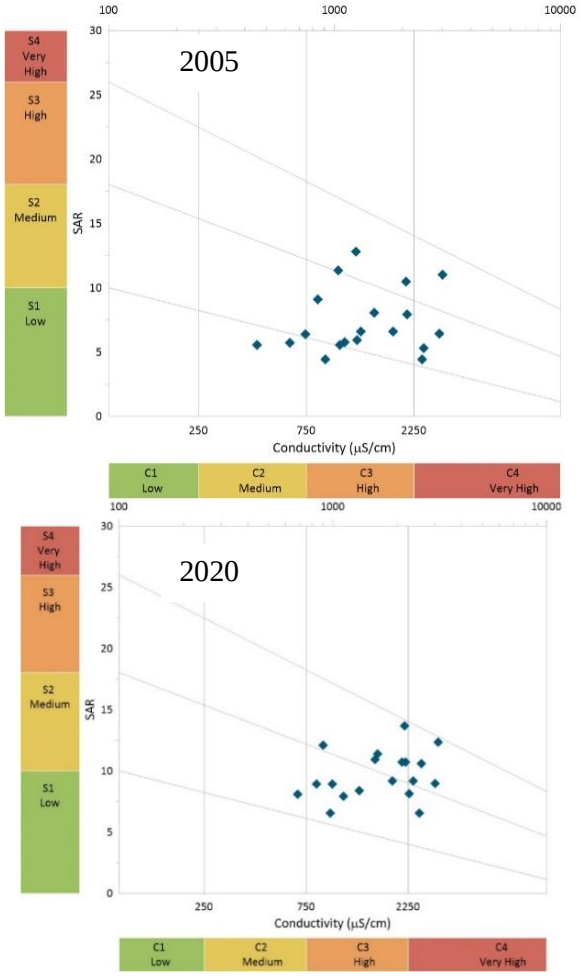

Fig. 6 USSL diagram in 2005 and 2020

According to the salinity hazard the majority of the samples were identified in the moderate salinity zone in 2005, but just a few samples were identified in this category in 2020. In contrast, the SAR values in 2005 and 2020 indicated that 55% of

the samples had low to medium sodium adsorption ratios. Salinity hazard and SAR estimates were correlated, and the results showed that 65% of the samples were moderately suitable for agriculture in 2005 and 35% in 2020, whereas 35% of the samples were deemed unsuitable for agriculture in 2005 and 65% in 2020.

3.5 Spatial variability map of groundwater level in the unconfined aquifer

One of the spatial interpolation techniques, ordinary kriging, is used to create the spatial variability maps of water table elevation and salinity that are shown in Figures 7 to 10. The maps can be used to comprehend the affected areas and rank them in terms of importance for incorporating various groundwater management plans into action. Three classes >2m, 2-4m, and >4m were used to define various groundwater level classes on the spatial maps. Based on the Central Pollution Control Board's classification, the area was divided into multiple EC classes (CPCB, 2018).

Pre-monsoon groundwater levels in both aquifers in 2005 ranged from -2 m to 3.6 m, and post-monsoon levels ranged from -0.4 m to 5.4 m. In the unconfined and semiconfined aquifers, a reverse hydraulic gradient is present during both seasons. This reveals that seawater intrusion has occurred here. In the research region of the Vadakara stretch, the issue is contained at a 5 km distance from the sea (Northern coast). The unconfined aquifer's groundwater level fluctuated over this stretch between -2 m and 0.37 m in the pre-monsoon and -0.43 to 1.2 m in the post-monsoon. During the pre-monsoon, the area of the semiconfined aquifer's negative groundwater elevation was 6 km from the sea. In both aquifers, the area covered by different groundwater elevation classes was listed in Table 2. In the unconfined aquifer, the area with groundwater elevation of less than 2 m class in 2005 was 24.4% in the pre-monsoon and 18.8% in the post-monsoon; by 2020, it was 28.7% and 21.5%, respectively. Similar patterns can be seen in the results from semiconfined aquifers. The recharge in both the aquifers during the monsoon may be responsible for the increase in groundwater level in the aquifer during post-monsoon.

Table 2 The delineated area under different water table elevation ranges

Aquifer	Water table elevation classes (m)	Area (%) 2005		Area (%) 2020	
		Pre-monsoon	Post-monsoon	Pre-monsoon	Post-monsoon
Unconfined	< 2	24.4	18.8	28.7	21.5
	2.0 - 4.0	39.3	51.6	39.1	44.9
	>4.0	36.3	29.6	32.2	33.6
Semiconfined	< 2	29.5	22.7	32.5	30.4
	2.0 - 4.0	38.4	48.8	37.9	44.7
	>4.0	32.1	28.5	29.6	24.9

Table 3 Delineated area under different Groundwater EC ranges

Aquifer	Groundwater EC classes (dS/m)	Area (%) 2005		Area (%) 2020	
		Pre-monsoon	Post-monsoon	Pre-monsoon	Post-monsoon
Unconfined	< 0.75	27	39.5	23.1	31.6
	0.75-2.25	28.2	43.5	31.7	44.5

	2.25-4	26.8	17	20	23.9
	>4.0	18	0	25.2	0
	< 0.75	26.5	41.2	20.1	20.6
Semiconfined	0.75-2.25	25.3	39.6	21.7	45.5
	2.25-4	29.3	19.2	33.6	33.9
	>4.0	18.9	0	24.6	0

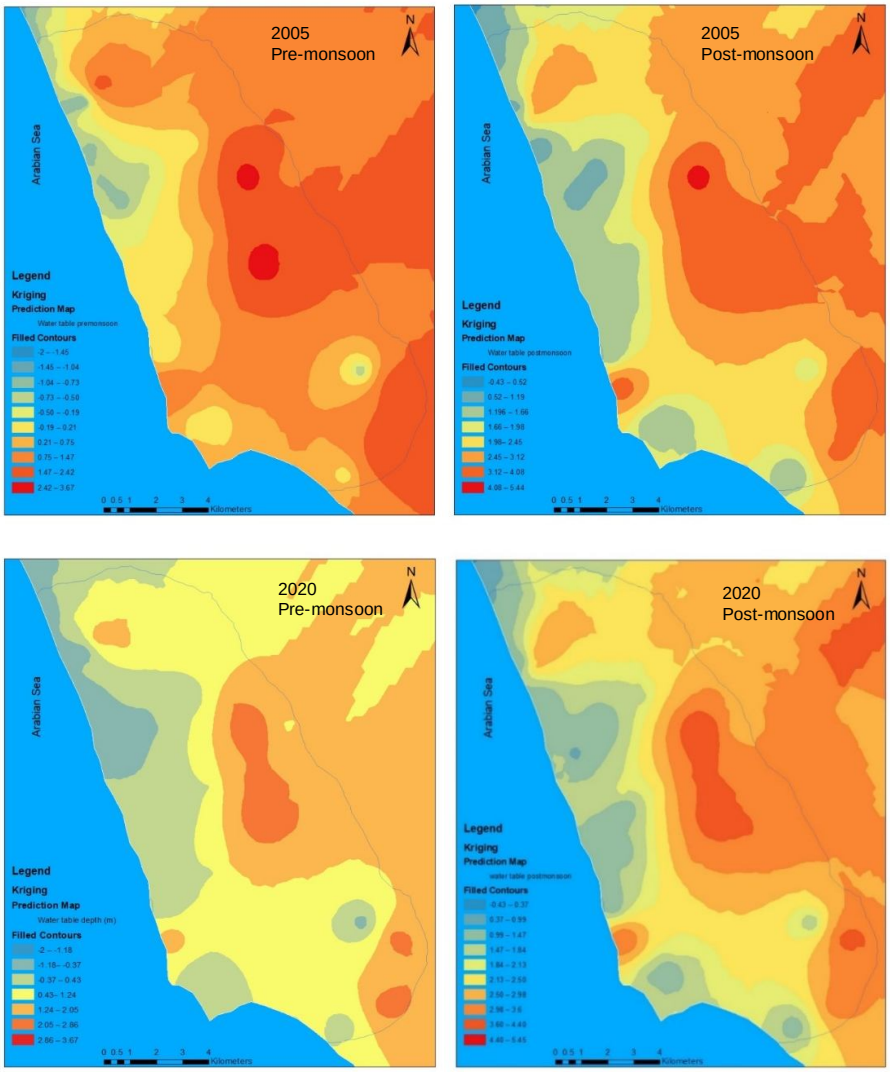

Fig. 7 Spatial variability map of the water table in the confined aquifer

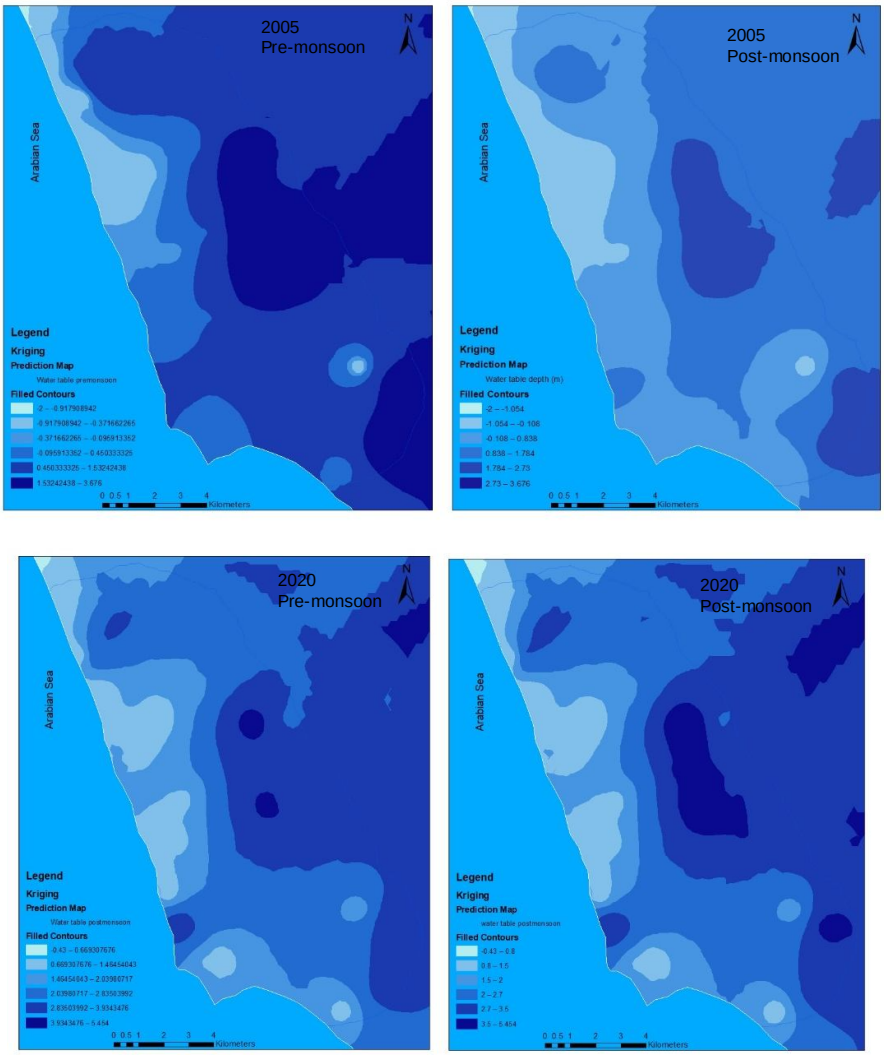

Fig. 8 Spatial variability map of the water table in the semi-confined aquifer

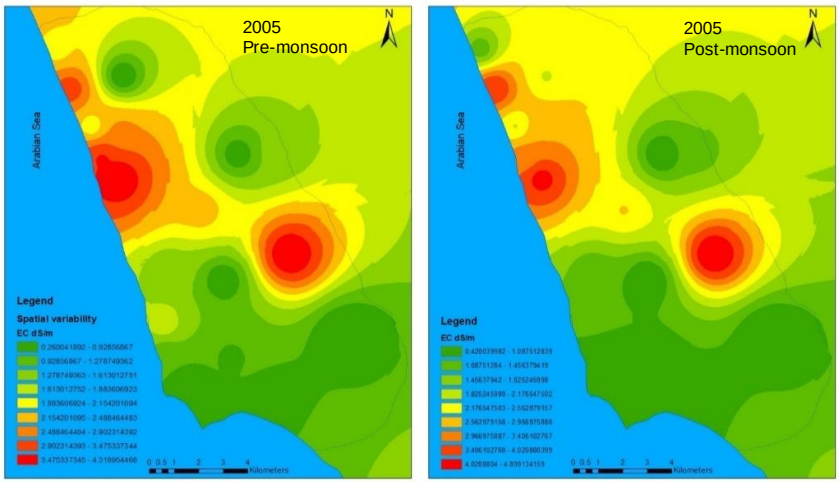

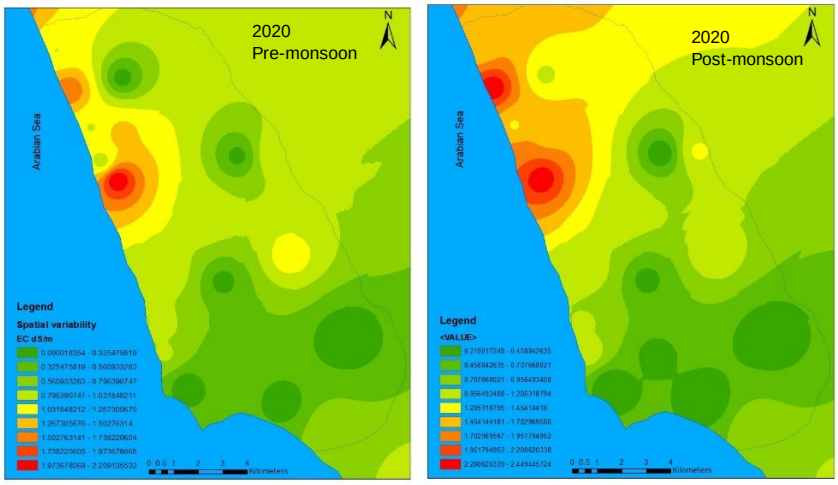

Fig. 9 Spatial variability map of the EC in the confined aquifer

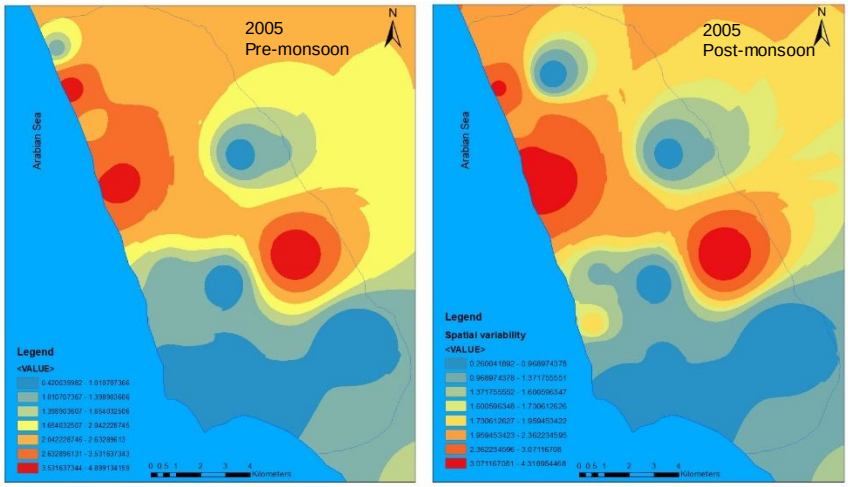

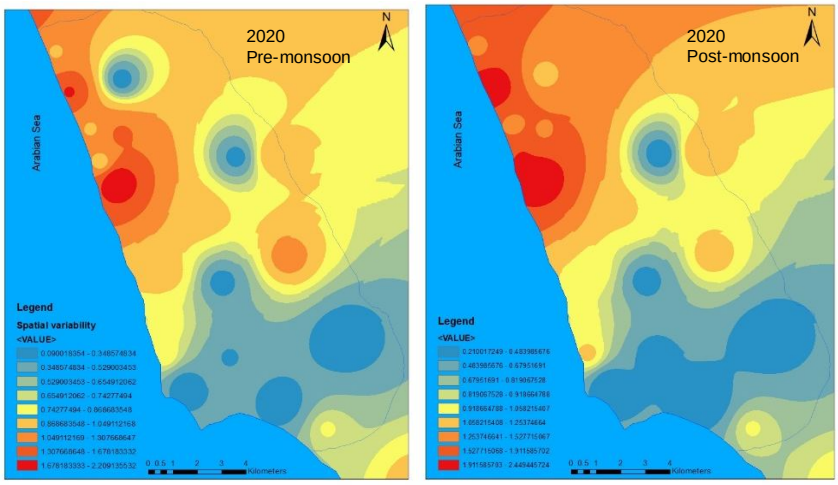

Fig. 10 Spatial variability map of the EC in the semi-confined aquifer

The spatial variation of salinity (Table 3) reveals that, in 2005, pre-monsoon, the EC of groundwater varies between 0.4 dS/m to 4.9dS/m in both the aquifers and in post-monsoon it varies between -0.2 dS/m to 2.4dS/m. The study area's northern coast shows higher EC than other regions. Along this stretch, the EC variation in the unconfined aquifer was between -2.9 dS/m to 4.8 dS/m in pre-monsoon and 1.5 dS/m to 2.2 dS/m in post-monsoon. Whereas in the semiconfined aquifer it ranges from 2.1 dS/m m to 4.1 dS/m m and in post-monsoon 1.1 dS/m to 2.2 dS/m. The area under various groundwater EC classes in both the aquifers (Table 3) shows that, in 2005, the area under groundwater EC less than 2.25 dS/m class in the unconfined aquifer was 55.2 % in pre-monsoon which increased to 83 % in post-monsoon whereas it was estimated as 54.8% and 76.1 % respectively in 2020. The area under groundwater EC greater than 4 dS/m class in the unconfined aquifer was 18 % in and 25.2 % in pre-monsoon in 2005 and 2020 respectively. However, in the post-monsoon, there is no area existing in this class. The recharging in the unconfined aquifer and recharging through the aquitard in the semiconfined aquifer during the monsoon may be responsible for the post-monsoon increase in groundwater quality. This might minimize the aquifer's reverse hydraulic gradient. The percentage of land classified as "unfit for irrigation" increased by 7% over the course of 15 years. The aquifer's declining groundwater level may increase the possibility of salt and freshwater mixing, which could account for the reduction in water quality over time.

4. Conclusion

The assessment of change in groundwater level and quality in the coastal aquifer of Kozhikode district in Kerala was done based on physical and chemical parameters, hydrogeochemical analysis, and spatial variations in groundwater levels and salinity for the period 2005-2020. Reduction in groundwater level and deterioration of groundwater quality premonsoon season in the study area were identified even though there is an increase in annual rainfall over the period. The change in Hydrochemical facies such as sulphates to chlorides in the anionic triangle and the spatial distribution of groundwater samples in the evaporation dominance zone in Gibbs plots reveal seawater intrusion into the wells. The irrigation water quality of 45 % of the groundwater samples was changed to high to very high salinity hazards in the aquifer during the 15 years. The groundwater level decreased during pre-monsoon thereby the seawater intrusion into the freshwater aquifers reduced the groundwater quality. However, the recharge of the aquifer from the monsoon improves the condition in post-monsoon. The results may be used for planning appropriate management strategies for managing the problem of seawater intrusion during the premonsoon season in this region.

References

Alfarrah, N., Walraevens, K., Farrah, N. al, and Martens, K. (2011). Hydrochemistry of the Upper Miocene-Pliocene-Quaternary aquifer complex of Jifarah Plain, NW-Libya. *Geologica Belgica*, *14*(3–4), 159–174.

Ali, S. A., and Ali, U. (2018). Hydrochemical characteristics and spatial analysis of groundwater quality in parts of Bundelkhand Massif, India. *Applied Water Science*, *8*(1).

Arslan, H. (2012). Spatial and temporal mapping of groundwater salinity using ordinary kriging and indicator kriging: The case of Bafra Plain, Turkey. *Agricultural Water Management*, *113*, 57–63.

CGWB. (2013). *Groundwater information booklet of Kozhikode district, Kerala state*.

Dash, C. J., Sarangi, A., and Singh, D. K. (2010). Spatial variability of groundwater depth and quality parameters in the National Capital Territory of Delhi. *Environmental Management*, *45*, 640–650.

Gibbs, R. J. (1970). Mechanisms Controlling World Water Chemistry. *Science*, *170*(3962), 1088–1090. https://doi.org/10.1126/science.170.3962.1088

Isaaks, E. H., and Srivastava, R. M. (1989). *An Introduction to Applied Geostatistics*. Oxford University Press.

KSPCB. (2019). *Report On Restoration of Polluted River Stretches Draft Action Plan Of River Kuttiyadi (Priority V)*.

Lanjwani, M. F., Khuhawar, M. Y., Jahangir Khuhawar, T. M., Samtio, M. S., and Memon, S. Q. (2021). Spatial variability and hydrogeochemical characterisation of groundwaters in Larkana of Sindh, Pakistan. *Groundwater for Sustainable Development*, *14*. https://doi.org/10.1016/j.gsd.2021.100632

Lanjwani, M. F., Khuhawar, M. Y., Lanjwani, A. H., Khuahwar, T. M. J., Samtio, M. S., Rind, I. K., Soomro, W. A., Khokhar, L. A., and Channa, F. A. (2022). Spatial variability and risk assessment of metals in groundwater of district Kamber-Shahdadkot, Sindh, Pakistan. *Groundwater for Sustainable Development*, 100784. https://doi.org/10.1016/j.gsd.2022.100784

Michalopoulos, D., and Dimitriou, E. (2018). Assessment of Pollution Risk Mapping Methods in an Eastern Mediterranean Catchment. *Journal of Ecological Engineering*, *19*, 55–68. https://doi.org/10.12911/22998993/79646

Nair, M. M. (1987). Coastal Geomorphology of Kerala. *Journal of The Geological Society of India*, *29*, 450–458.

Nazimuddin, M. (1993). *Coastal Hydrogeology of Kozhikode, Kerala Under the Faculty Of Marine Sciences*.

Piper, A. M. (1944). A graphic procedure in the geochemical interpretation of water-analyses. *Transactions, American Geophysical Union*, *25*(6), 914. https://doi.org/10.1029/TR025i006p00914

Rao, N. S., Vidyasagar, G., Surya Rao, P., and Bhanumurthy, P. (2017). Chemistry and quality of groundwater in a coastal region of Andhra Pradesh, India. *Applied Water Science*, *7*(1), 285–294. https://doi.org/10.1007/s13201-014-0244-0

Richards, L. A. (1954). *Diagnosis and Improvement of Saline and Alkali Soils, Agricultural Handbook* (Vol. 60). US Department of Agriculture.

Salaj, S. S., Ramesh, D., Suresh Babu, D. S., and Kaliraj, S. (2018). *Impacts of urbanization on groundwater vulnerability along the Kozhikode coastal stretch, Southwestern India using GIS based modified DRASTIC-U Model*. www.jcsonline.co.nr

Sangadi, P., Kuppan, C., and Ravinathan, P. (2022). Effect of hydro-geochemical processes and saltwater intrusion on groundwater quality and irrigational suitability assessed by geo-statistical techniques in coastal region of eastern Andhra Pradesh, India. *Marine Pollution Bulletin*, *175*. https://doi.org/10.1016/j.marpolbul.2022.113390

Sathiamoorthy, M., and Ganesan, M. (2018). *Hydro geochemical characterization of surface and groundwater quality and assessing its suitability of drinking and irrigational purposes in Veeranam tank area, Cuddalore district, Tamil Nadu, India*. *23*.

Shin, K., Koh, D. C., Jung, H., and Lee, J. (2020). The hydrogeochemical characteristics of groundwater subjected to seawater intrusion in the Archipelago, Korea. *Water (Switzerland)*, *12*(6). https://doi.org/10.3390/W12061542

Zhang, B., Zhao, D., Zhou, P., Qu, S., Liao, F., and Wang, G. (2020). Hydrochemical characteristics of groundwater and dominantwater-rock interactions in the Delingha area, Qaidam Basin, Northwest China. *Water (Switzerland)*, *12*(3). https://doi.org/10.3390/w12030836